



Unveiling the Interplay Between Diffusing CO₂ and Ethanol Molecules in Champagne Wines by Classical Molecular Dynamics and ¹³C NMR Spectroscopy

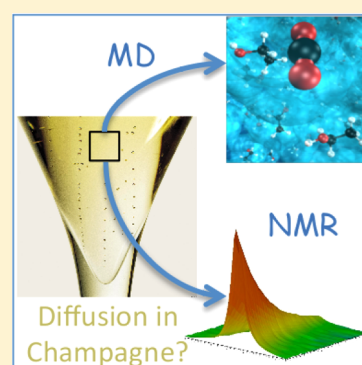
David A. Bonhommeau,^{*,†} Alexandre Perret,[†] Jean-Marc Nuzillard,^{*,‡} Clara Cilindre,[†] Thibaud Cours,[†] Alexander Alijah,[†] and Gérard Liger-Belair[†]

[†]GSMA, UMR CNRS 7331, Université de Reims Champagne-Ardenne, Campus Moulin de la Housse BP 1039, 51687 Reims Cedex 2, France

[‡]ICMR, UMR CNRS 7312, Université de Reims Champagne-Ardenne, Campus Moulin de la Housse BP 1039, 51687 Reims Cedex 2, France

S Supporting Information

ABSTRACT: The diffusion coefficients of carbon dioxide (CO₂) and ethanol (EtOH) in carbonated hydroalcoholic solutions and Champagne wines are evaluated as a function of temperature by classical molecular dynamics (MD) simulations and ¹³C NMR spectroscopy measurements. The excellent agreement between theoretical and experimental diffusion coefficients suggest that ethanol is the main molecule, apart from water, responsible for the value of the CO₂ diffusion coefficients in typical Champagne wines, a result that could likely be extended to most sparkling wines with alike ethanol concentrations. CO₂ and EtOH hydrodynamical radii deduced from viscometry measurements by applying the Stokes–Einstein relationship are found to be mostly constant and in close agreement with MD predictions. The reliability of our approach should be of interest to physical chemists aiming to model transport phenomena in supersaturated aqueous solutions or water/alcohol mixtures.



SECTION: Liquids; Chemical and Dynamical Processes in Solution

Carbon dioxide (CO₂) supersaturation occurs in a wide variety of aqueous multicomponent systems from inland waters and brines to sparkling beverages. Inland waters such as rivers, lakes, and wetlands are often supersaturated with CO₂ and play a major role in the evasion of petagrams of CO₂ into the atmosphere, then contributing to the global carbon cycle.^{1–3} Evaluating the yields of CO₂ evasion by temperature, alkalinity, and pH measurements coupled to morphological studies of the wide surface areas from which CO₂ escapes thus allows to rationalize better the anthropogenic contribution to CO₂ emissions with respect to natural sources of CO₂ production. CO₂ emission at the interface between a supersaturated aqueous solution and a gas phase is also one of the two physical phenomena accounting for the loss of CO₂ in sparkling beverages such as Champagne wines.⁴ The second path to CO₂ emission in carbonated beverages is related to the very much sought after and so-called effervescence process. Effervescence refers to the formation of bubbles by nonclassical heterogeneous nucleation from tiny gas pockets trapped within immersed particles such as cellulose fibers, crystals, or within possible scratches or etchings done at the surface of the glass.⁵ Provided that the radius of curvature of the gas pocket trapped within the particle exceeds a critical radius (of order of 0.2 μm at the opening of a champagne bottle), the diffusion of dissolved CO₂ within the gas pocket becomes thermodynamically

possible. Gaseous CO₂ bubbles therefore progressively grow within the particle, to finally be released in the champagne bulk into the form of characteristic bubble trains.⁵ Force field molecular dynamics simulations based on TIP5P water models have recently suggested that CO₂ diffusion coefficients at *T* = 293 K could be predicted⁶ by simply modeling champagne as a hydroalcoholic solution supersaturated with CO₂. Although the approach followed by the authors could be applicable to a wide range of liquids supersaturated with gases (eg, CO₂, methane, etc.), the SPC/E water model, supposed to be reliable for modeling the diffusion of CO₂ in water^{6–8} and sometimes used to model water/alcohol mixtures,⁹ was found to strongly underestimate CO₂ diffusion coefficients. Moreover, comparative diffusion coefficients of dissolved CO₂ in various carbonated beverages (including a standard Champagne wine) were only determined through the nuclear magnetic resonance (NMR) technique at a single temperature of 293 K.¹⁰ A thorough temperature-dependent study would therefore be valuable for both evaluating the performance of MD simulations to model such systems and better apprehending the

Received: September 24, 2014

Accepted: November 13, 2014

Published: November 13, 2014



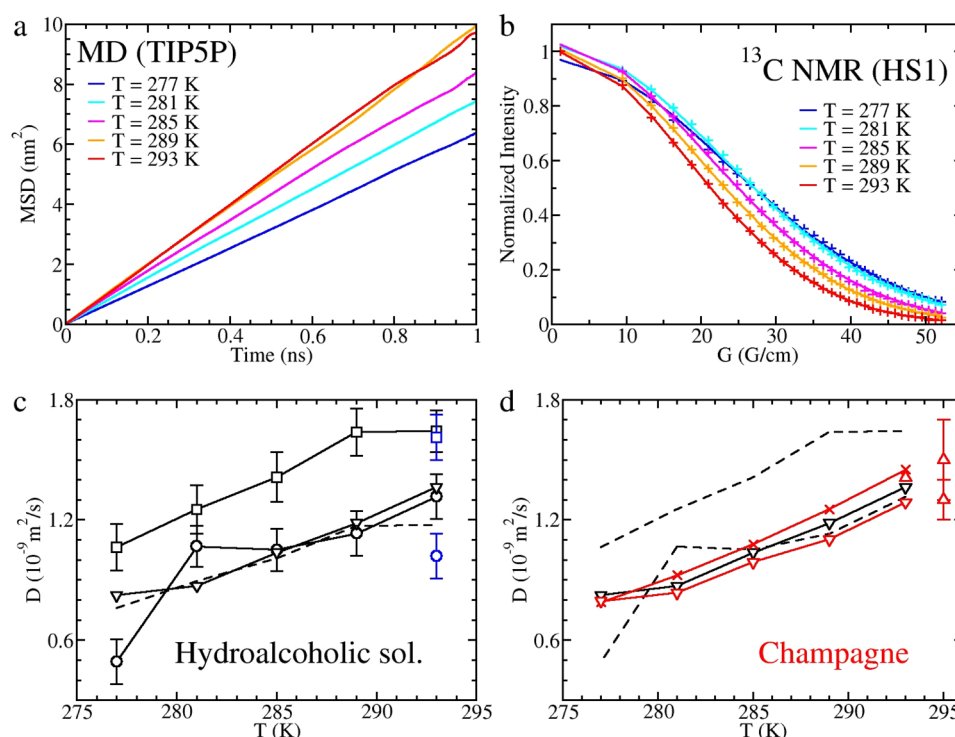


Figure 1. (a) Mean squared displacements (MSDs) of CO₂ centers of mass in a carbonated TIPSP water/ethanol mixture at temperatures ranging from 277 to 293 K. (b) ¹³C NMR peak position of ¹³CO₂ in a carbonated hydroalcoholic sample (HS1) at temperatures ranging from 277 to 293 K. The plus signs represent experimental data points whose nonlinear fit is depicted as a solid curve. (c) CO₂ diffusion coefficients in carbonated hydroalcoholic solutions deduced from TIPSP MD runs (black squares), SPC/E MD runs (black circles), and ¹³C NMR spectroscopy measurements (black downward triangles). The blue symbols represent TIPSP and SPC/E results from the literature.⁶ The dashed line is obtained by dividing the TIPSP curve by an empirical factor of 1.4. (d) CO₂ diffusion coefficients in common Champagne wines deduced from ¹³C NMR spectroscopy measurements (red downward triangles), NMR spectroscopy measurements from the literature (red upward triangles),^{10,14} and the Stokes–Einstein relationship of eq 1 (red crosses). The dashed curves refer to the TIPSP and SPC/E diffusion coefficients plotted in panel c.

influence of temperature on bubble dynamics and subsequently on some tasting sensations.

The main goal of this work is to characterize the interplay between CO₂ and ethanol (EtOH) molecules in standard Champagne wines as a function of temperature in order to demonstrate that EtOH is the principal molecule responsible for the value of CO₂ diffusion coefficients in these multicomponent liquids. This assertion is supported by extensive classical molecular dynamics (MD) simulations and ¹³C NMR spectroscopy measurements that aim to evaluate CO₂ and EtOH diffusion coefficients. These diffusion coefficients, combined to experimental and theoretical viscosities, will also be shown to provide CO₂ and EtOH hydrodynamical radii that nearly match the root-mean-squared (rms) atomic distance to the molecular center of mass, which promises a wide applicability of our approach.

Our MD simulations make use of GROMACS version 4.5.5¹¹ coupled to the CHARMM27 force field.¹² Despite their multicomponent nature, champagnes can be considered as carbonated hydroalcoholic mixtures in first approximation.^{5,6} The simulation box then contains 10 000 water molecules, described within the SPC/E or TIPSP water model, 440 ethanol molecules and 50 CO₂ molecules, reflecting the typical molecular proportions in Champagne wines.^{5,13} [Champagnes typically hold 12.5% vol/vol of ethanol and 12 g/L of dissolved CO₂ (following the so-called Henry's law which states that the equilibrium concentration of dissolved CO₂ is proportional to the partial pressure of gas phase CO₂).] Sugars are neglected in the present simulations since we focus our discussion on

standard commercial champagnes, namely brut champagnes (<12g/L of sugars, that is, a maximum of six saccharose molecules in our simulation box) that roughly represent 83% of worldwide exportations (a pie chart representing 2013 Champagne wine shipments is provided in page S2 of the Supporting Information). Simulations at five temperatures relevant for applications on Champagne wines, namely 277 K (fridge temperature), 281 and 285 K (cellar and tasting temperature), and 289 and 293 K (room temperature), are performed and subsequently used for evaluating CO₂ and EtOH diffusion coefficients (additional details concerning MD simulations are supplied in pages S1–S3 of the Supporting Information). These coefficients are derived from the calculation of the mean-squared displacement (MSD) of CO₂ and EtOH centers of mass in a three-dimensional space, $MSD(t) = 6Dt$, then assuming that the CO₂ and EtOH fluxes can be represented by common first Fick's laws with effective diffusion coefficients that encompass the effects of CO₂ and EtOH concentration gradients. As illustrated in Figure 1a for MD simulations based on the TIPSP water model, MSD curves obtained for CO₂ molecules are almost perfectly linear at any temperature (the MSD curves corresponding to SPC/E water models are given on page S3 of the Supporting Information), which confirms that the probability density of CO₂ molecules should be Gaussian and therefore validates the assumption made on the expression of fluxes in terms of effective diffusion coefficients.

In order to evaluate unambiguously the quality of TIPSP and SPC/E MD simulations, translational diffusion coefficients

were measured by ^{13}C NMR spectroscopy in a model mixture (87.5:12.5 (v/v) $\text{H}_2\text{O}:\text{EtOH}$) and in a standard commercial brut Champagne wine sample (Veuve Clicquot, Marne, France). Our highly sensitive spectrometer, with a large magnetic field ($B = 14\text{T}$) and a state-of-the-art cryoprobe (coil at $T = 20\text{K}$), is well suited for providing reliable measurements over a broad range of temperatures and discussing the accuracy of previous NMR measurements^{10,14} (details on the NMR protocol and NMR data are given in pages S3–S6 of the Supporting Information). It is also worth noting that no CO_2 bubble, which might bias experimental measurements, can form in NMR tubes. Indeed, a large amount of dissolved CO_2 is lost through outgassing when filling sample tubes with native champagne, so that dissolved CO_2 concentration most probably falls below the critical concentration, enabling heterogeneous bubble nucleation.¹⁵ This loss of CO_2 is somewhat compensated by the addition of $\text{NaH}^{13}\text{CO}_3$, then improving at the same time the ^{13}C NMR signal. Due to the weak interactions between the relatively rare (0.5% of the total number of molecules) nonpolar CO_2 molecules, we assume in NMR experiments that deviations due to smaller CO_2 concentrations should lie below experimental uncertainties ($\sim 5\%$, the size of symbols in Figure 1). As illustrated in Figure 1b for a sample containing a carbonated hydroalcoholic solution, diffusion coefficients are then determined by fitting a series of 32 intensities of $^{13}\text{CO}_2$ signals at each temperature of interest.

Diffusion coefficients derived from ^{13}C NMR spectroscopy measurements in carbonated hydroalcoholic solutions (black downward triangles in Figure 1c) are found in excellent agreement with SPC/E results above 281 K. The SPC/E model is a reparameterization of the SPC model that includes polarization effects in order to improve the reliability of water properties, such as radial distributions, diffusion constants and densities, at temperatures about 300–305 K.¹⁶ It is therefore not expected to reproduce the water density maximum at $T = 277\text{ K}$ much better than the standard SPC model. On the contrary, the TIPSP model was devised to better reproduce water density at this temperature.¹⁷ Although TIPSP diffusion coefficients overestimate experimental data by 30–40%, they are perfectly parallel to the experimental curve, even at low temperature, and a simple division of these coefficients by an empirical factor of 1.4 (dashed line in Figure 1c), in order to compensate the excessive TIPSP diffusivity, significantly improves the agreement with experiments at $277\text{ K} \leq T \leq 289\text{ K}$. This overestimation can be partly related to results obtained on water self-diffusion coefficients,¹⁸ where the TIPSP diffusion coefficient ($D = 2.62 \pm 0.04 \times 10^{-9}\text{ m}^2/\text{s}$) was found to slightly overestimate the experimental value ($D = 2.3 \times 10^{-9}\text{ m}^2/\text{s}$) and the diffusion coefficient predicted by the SPC/E model ($D = 2.49 \pm 0.05 \times 10^{-9}\text{ m}^2/\text{s}$) at $T = 298\text{ K}$. A slight overestimation has also been recently observed at $T = 293\text{ K}$ for CO_2 diffusion in water,⁶ where the TIPSP diffusion coefficient ($D = 2.36 \pm 0.09 \times 10^{-9}\text{ m}^2/\text{s}$) was $\sim 12\%$ higher than the SPC/E diffusion coefficient ($D = 2.11 \pm 0.14 \times 10^{-9}\text{ m}^2/\text{s}$). However, we cannot exclude the fact that our model for ethanol, based on the CHARMM27 force field, is also in part responsible for this overestimation. Based on these observations, we would recommend the SPC/E model for evaluating diffusion coefficients in such aqueous solutions at temperatures $285\text{ K} \leq T \leq 300\text{ K}$ (higher temperatures are not relevant for wine research, especially when considering sparkling beverages) and the TIPSP model at lower temperatures, provided that one

SPC/E or experimental value of diffusion coefficient is available at higher temperature to estimate any possible scaling factor.

The impressively good agreement obtained above 281 K when the SPC/E model is used also contrasts with the poor agreement obtained with this model in previous studies at $T = 293\text{ K}$ (blue circle in Figure 1c).⁶ The newly gained reliability seems to come from an improved equilibration stage where standard canonical (NVT) equilibrations are replaced by replica exchange molecular dynamics (REMD) simulations in the isothermal–isobaric (NPT) ensemble. Without any REMD simulation, the average enthalpy of the system is indeed $-4.14 \pm 0.2 \times 10^5\text{ kJ/mol}$, whereas it increases to $-4.09 \pm 0.2 \times 10^5\text{ kJ/mol}$ as a REMD equilibration stage is performed, a difference that was identified to be mainly due to smaller Coulomb short-range interactions in the former simulation. In contrast, the average enthalpy for systems with TIPSP water molecules (black and blue squares in Figure 1c) remains ca. $-3.51 \times 10^5\text{ kJ/mol}$ when replica exchange equilibrations are performed. Knowing that no major energy barrier should exist in our model carbonated hydroalcoholic solution, the discrepancy observed in former SPC/E simulations probably came from an incomplete equilibration stage that might have been overcome by performing longer NPT simulations.

CO_2 diffusion coefficients derived from ^{13}C NMR measurements on typical brut champagnes (red downward triangles in Figure 1d) are found to nearly match experimental CO_2 diffusion coefficients obtained in carbonated hydroalcoholic solutions, with a gap between the two curves that does not exceed $0.8 \times 10^{-10}\text{ m}^2/\text{s}$. These coefficients are also in very close agreement with diffusion coefficients estimated by applying the Stokes–Einstein formula (red crosses in Figure 1d)

$$D = \frac{k_B T}{6\pi\eta R} = \frac{k_B T}{6\pi R (1.08 \times 10^{-7} e^{2806/T})} \quad (1)$$

where k_B is the Boltzmann constant, T (K) is the temperature, η (Pa·s) is the viscosity that follows an Arrhenius-like law adjusted on viscometry measurements performed on standard commercial champagne (from coopérative Nogent l'Abbesse, Marne, France),¹⁹ and R (m) is the hydrodynamical radius of the diffusing molecule that is assumed to roughly match the rms atomic distance to the CO_2 center of mass ($R_{\text{CO}_2} \approx 0.95\text{ \AA}$ in our simulations) deduced from MD simulations. The good correspondence between the values of CO_2 diffusion coefficients obtained for champagne wines and carbonated hydroalcoholic solutions indicates that glycerol molecules and sugars, the next more abundant species that could increase the viscosity of champagnes, probably have minor effect on the value of CO_2 diffusion coefficients. Ethanol is therefore the main molecule, apart from water, responsible for the value of the CO_2 diffusion coefficient, although champagne is a multicomponent mixture composed of a large number of species, from monatomic ions to sugars and macromolecules. The previous results then confirm that modeling champagnes as carbonated hydroalcoholic solutions by using common water models is sufficient to capture most of the physical effects involved in CO_2 diffusion in these systems.

As illustrated in Figure 2a, SPC/E and TIPSP EtOH diffusion coefficients essentially surround the diffusion coefficients deduced from ^{13}C NMR measurements on carbonated hydroalcoholic solutions. The TIPSP model remains more accurate than the SPC/E model at low

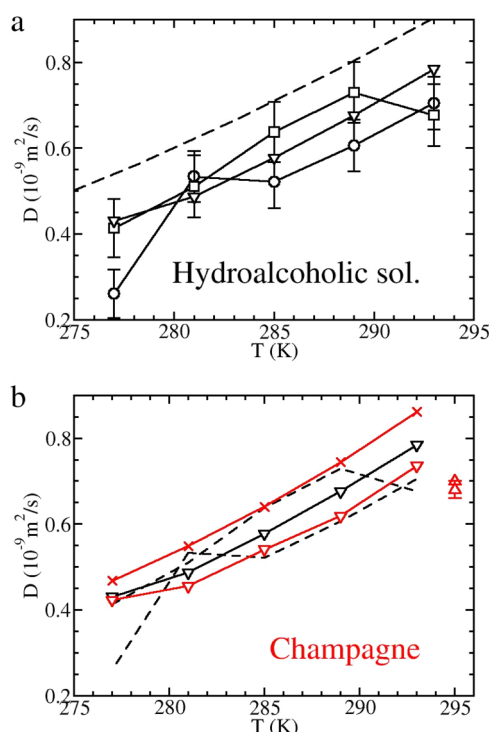


Figure 2. (a) EtOH diffusion coefficients in carbonated hydroalcoholic solutions deduced from TIPSP MD runs (black squares), SPC/E MD runs (black circles), and ^{13}C NMR spectroscopy measurements (black downward triangles). The dashed curve represents empirical results for the infinite dilution of EtOH in pure water.^{20,21} (b) EtOH diffusion coefficients in common Champagne wines deduced from ^{13}C NMR spectroscopy measurements (red downward triangles), NMR spectroscopy measurements from the literature at 295 K (red upward triangles),¹⁴ and the Stokes–Einstein relationship of eq 1 (red crosses). The dashed curves refer to the TIPSP and SPC/E diffusion coefficients plotted in panel a.

temperature, and we can check that all these curves lie roughly $0.1\text{--}0.2 \times 10^{-9} \text{ m}^2/\text{s}$ below empirical diffusion coefficients obtained for infinitely diluted ethanol in water, the upper limit that EtOH diffusion coefficients should not exceed since ethanol increases the viscosity of liquids, over the full temperature range from 277 to 293 K (dashed line in Figure 2a). From a quantitative point of view, EtOH diffusion coefficients are roughly half as big as CO_2 diffusion coefficients, and differences between SPC/E and TIPSP models seem softened, whereas their overall mixture enthalpy differs by $\sim 14\%$. This unexpected behavior can be partly explained in terms of the average number of H bonds (H bonds are defined by purely geometric considerations^{6,22} based on the “g_hbond” tool supplied in the GROMACS version 4.5.5 distribution) per molecule, which hardly reaches 0.3–0.5 for CO_2 but increases to 2.5–2.7 for EtOH, over the whole temperature range investigated here. Consequently, CO_2 rather diffuses as a spectator species in the network formed by water and EtOH molecules, a behavior already postulated elsewhere,⁶ and it is strongly influenced by stability alterations of the hydroalcoholic mixture. A drop in enthalpy, as observed with the TIPSP water model, will yield a smaller “caging” of CO_2 molecules and a possible increase of their diffusivity (see Figure 1c). On the contrary, EtOH molecules form more H bonds with their environment, their diffusivity is decreased compared to CO_2 molecules, and differences in water models have weaker

dynamic effects on these less mobile species (see Figure 2a). The small shift of $0.1\text{--}0.5 \times 10^{-10} \text{ m}^2/\text{s}$ between ^{13}C NMR measurements performed in carbonated hydroalcoholic solutions (black downward triangles in Figure 2b) and Champagne wines (red downward triangles in Figure 2b) also reveals that the value of EtOH diffusion coefficients should not be influenced significantly by molecules other than water and CO_2 in brut champagnes. MD-based diffusion coefficients essentially lie in between semiempirical diffusion coefficients based on eq 1 with $R_{\text{EtOH}} \approx 1.6 \text{ \AA}$ (red crosses in Figure 2b) and NMR spectroscopy measurements (red downward and upward triangles in Figure 2b). With regard to experimental and theoretical uncertainties, all these diffusion coefficients can therefore be considered to be in very close agreement.

It is a matter of fact that diffusion coefficients in sparkling beverages can be easily determined from viscosities by applying the Stokes–Einstein relationship (see eq 1) provided that the hydrodynamical radii of diffusing molecules are known. In a previous work,⁶ we found that simply defining the CO_2 hydrodynamical radius as the rms atomic distance to the CO_2 center of mass was sufficient to reproduce the typical viscosity of champagnes at $T = 293 \text{ K}$, but the validity of this empirical definition was not evaluated at lower temperatures and for larger molecules. We first report in Table 1 theoretical

Table 1. Viscosities ($10^{-3} \text{ Pa}\cdot\text{s}$) of Hydroalcoholic Solutions and Champagne Wines as a Function of Temperature ($277 \text{ K} \leq T \leq 293 \text{ K}$) for the Mixtures Considered in MD Simulations (Columns 2 and 3) and for Hydroalcoholic Samples (HS) and Champagne Samples (CS) Typically Used in ^{13}C -NMR Measurements (Columns 4 and 5)^a

$T \text{ (K)}$	$\eta_{\text{SPC/E}}$	η_{TIPSP}	η_{HS}	η_{CS}	η_{CL}
277	2.46 ± 0.84	1.56 ± 0.01	2.602	2.885	2.709
281	1.89 ± 0.65	1.35 ± 0.01	2.245	2.460	2.345
285	1.48 ± 0.33	1.75 ± 0.46	1.955	2.136	2.039
289	1.63 ± 0.42	1.15 ± 0.18	1.718	1.856	1.779
293	1.32 ± 0.33	1.26 ± 0.19	1.523	1.636	1.558

^aColumn 6 reports brut champagne viscosities from the literature (CL).²³

viscosities calculated from MD simulations by evaluating the transverse current autocorrelation functions (we used the g_tcaf GROMACS tool for this purpose), dynamical viscosities deduced from viscometry measurements (details on these experiments are given in pages S4 and S5 of the Supporting Information), and viscosities from the literature.²³ Despite the large uncertainties, SPC/E viscosities are in good agreement with dynamical viscosities measured in hydroalcoholic solutions. TIPSP viscosities are underestimated as expected from the overestimation of CO_2 , and to a lesser extent EtOH, diffusion coefficients when this water model is used. Both viscosities measured on brut champagnes lie above the viscosity of the hydroalcoholic solution and they only differ by $\sim 5\%$, a deviation that can be attributed to the composition of these two sparkling beverages and to experimental uncertainties. The dynamical viscosities are then combined with ^{13}C NMR CO_2 and EtOH diffusion coefficients to provide an experimental estimate of the CO_2 and EtOH hydrodynamical radii from the Stokes–Einstein relationship. Table 2 compares these experimental estimations of hydrodynamical radii with theoretical radii derived from MD diffusion coefficients and viscosities at $277 \text{ K} \leq T \leq 293 \text{ K}$. Experimental hydrodynamical radii are

Table 2. Hydrodynamical Radii (Å) of CO₂ and EtOH Obtained by Applying the Stokes–Einstein Relationship^a

T (K)	CO ₂				EtOH			
	$R_{\text{SPC/E}}$	R_{TIP5P}	R_{HS}	R_{CS}	$R_{\text{SPC/E}}$	R_{TIP5P}	R_{HS}	R_{CS}
277	1.68 ± 0.96	1.22 ± 0.14	0.95	0.88	3.16 ± 1.76	3.14 ± 0.54	1.81	1.66
281	1.02 ± 0.45	1.22 ± 0.13	1.05	1.00	2.04 ± 0.93	2.98 ± 0.44	1.88	1.83
285	1.34 ± 0.44	0.84 ± 0.30	1.03	0.99	2.70 ± 0.92	1.87 ± 0.70	1.85	1.81
289	1.15 ± 0.41	1.12 ± 0.26	1.04	1.03	2.14 ± 0.76	2.52 ± 0.64	1.82	1.84
293	1.24 ± 0.41	1.04 ± 0.22	1.03	1.02	2.31 ± 0.78	2.52 ± 0.65	1.80	1.78

^a $R_{\text{SPC/E}}$ and R_{TIP5P} are deduced from the theoretical diffusion coefficients and viscosities that correspond to MD simulations including SPC/E and TIP5P water molecules, respectively. R_{HS} and R_{CS} are deduced from ¹³C-NMR diffusion coefficients and viscometry measurements on carbonated hydroalcoholic samples (HS) and champagne samples (CS). Experimental uncertainties are estimated to remain below 0.04 Å.

little temperature-dependent ($R_{\text{CO}_2} \approx 1$ Å and $R_{\text{EtOH}} \approx 1.8$ Å) and they only decrease by 1% to 10% in champagnes compared to carbonated hydroalcoholic solutions. Their deviation from the empirical rms estimates ($R_{\text{CO}_2} \approx 0.95$ Å and $R_{\text{EtOH}} \approx 1.6$ Å) does not exceed ~10% for CO₂ and ~18% for EtOH, and the agreement with theoretical hydrodynamical radii, namely $R_{\text{SPC/E}}$ and R_{TIP5P} , is also qualitatively correct. This confirms the suitability of our simple definition of hydrodynamical radii for relatively small diffusing molecules and the relevance of the Stokes–Einstein relationship for evaluating viscosities or diffusion coefficients in supersaturated aqueous solutions such as Champagne wines.

In this Letter we compared CO₂ and EtOH diffusion coefficients deduced from classical molecular dynamics simulations, ¹³C NMR spectroscopy measurements, and semiempirical formulas based on an Arrhenius-like law to unveil the interplay between CO₂ and EtOH molecules in Champagne wines. We showed that experimental and theoretical diffusion coefficients are in very close agreement to each other and that carbonated hydroalcoholic solutions can be considered as proper models to investigate CO₂ and EtOH diffusion in Champagne wines. In particular, EtOH was shown to be the main molecule responsible for the value of CO₂ diffusion coefficients in these beverages, and probably in most sparkling wines with alike ethanol concentrations provided that sugars are not in large amount in the solution, which is true for standard commercial champagnes, namely brut champagnes. In other words, there should be no major correlation between the taste of such sparkling wines, mainly due to acids, sugars, and proteins in the mixture, and the formation and growth dynamics of CO₂ bubbles that mainly relies on CO₂ diffusion. Moreover, CO₂ diffusion seems more sensitive to alterations in water models than EtOH molecules, a property that was partly attributed to the larger propensity of EtOH molecules to participate in the H bonding network, making these molecules less mobile by nature and therefore less prone to dynamic changes. CO₂ and EtOH hydrodynamical radii deduced from the insertion of theoretical or experimental viscosities in the Stokes–Einstein relationship were also found to be in good agreement with the predictions given by the rms atomic distance to molecular centers of mass. This simple empirical definition of hydrodynamical radii could therefore be used as first approximation to evaluate diffusion coefficients or viscosities in liquids, and especially in water/alcohol mixtures commonly used as solvents in physical chemistry.

■ ASSOCIATED CONTENT

Supporting Information

Theoretical details on classical MD simulations (MD protocol, table with the model mixture properties, supplementary MSD curves for CO₂ and EtOH, tables with diffusion coefficients), empirical model from the literature, experimental details on ¹³C NMR spectroscopy measurements (sample preparation and additional ¹³C NMR data curves) and viscometry measurements (table with experimental densities and kinematic viscosities). This material is available free of charge via the Internet at <http://pubs.acs.org>.

■ AUTHOR INFORMATION

Corresponding Authors

*E-mail: david.bonhommeau@univ-reims.fr; Phone: +33 (0)3 26 91 33 33. Fax: +33 (0)3 26 91 31 47.

*E-mail: jean-marc.nuzillard@univ-reims.fr.

Notes

The authors declare no competing financial interest.

■ ACKNOWLEDGMENTS

The authors are indebted to the Bull company for financial support through ANRT grant 2011/1288 and to Alain Cornu for freely providing us with the champagne glass photograph included in the TOC graphic. The “Très Grand Centre de Calculs” (TGCC) of the “Grand Equipement National de Calcul Intensif” (GENCI), the ROMEO computer center of the Champagne-Ardenne region, and the “Plateau technique de Modélisation Moléculaire Multiéchelle” in Reims (P3M), are gratefully acknowledged for computer resources and technical support. The authors warmly thank Champagne Veuve Clicquot for supplying us with champagne samples. Financial supports by CNRS, Conseil Regional Champagne Ardenne, Conseil General de la Marne, Ministry of Higher Education and Research (MESR), EU-programme FEDER to the PIAnET CPER project, and Association Recherche Oenologie Champagne Université (AROCU) are also gratefully acknowledged.

■ REFERENCES

- (1) Mayorga, E.; Aufdenkampe, A. K.; Masiello, C. A.; Krusche, A. V.; Hedges, J. I.; Quay, P. D.; Richey, J. E.; Brown, T. A. Young Organic Matter as a Source of Carbon Dioxide Outgassing from Amazonian Rivers. *Nature* **2005**, *436*, 538–541.
- (2) Butman, D.; Raymond, P. A. Significant Efflux of Carbon Dioxide from Streams and Rivers in the United States. *Nat. Geosci.* **2011**, *4*, 839–842.
- (3) Raymond, P. A.; Hartmann, J.; Lauerwald, R.; Sobek, S.; McDonald, C.; Hoover, M.; Butman, D.; Striegl, R.; Mayorga, E.; Humborg, C.; et al. Global Carbon Dioxide Emissions from Inland Waters. *Nature* **2013**, *503*, 355–359.

- (4) Liger-Belair, G.; Villaume, S.; Cilindre, C.; Polidori, G.; Jeandet, P. CO₂ Volume Fluxes Outgassing from Champagne Glasses in Tasting Conditions: Flute versus Coupe. *J. Agric. Food Chem.* **2009**, *57*, 4939–4947.
- (5) Liger-Belair, G.; Polidori, G.; Jeandet, P. Recent Advances in the Science of Champagne Bubbles. *Chem. Soc. Rev.* **2008**, *37*, 2490–2511.
- (6) Perret, A.; Bonhommeau, D. A.; Liger-Belair, G.; Cours, T.; Alijah, A. CO₂ Diffusion in Champagne Wines: A Molecular Dynamics Study. *J. Phys. Chem. B* **2014**, *118*, 1839–1847.
- (7) Zeebe, R. E. On the Molecular Diffusion Coefficients of Dissolved CO₂, HCO₃⁻, and CO₃²⁻ and Their Dependence on Isotopic Mass. *Geochim. Cosmochim. Acta* **2011**, *75*, 2483–2498.
- (8) In Het Panhuis, M.; Patterson, C. H.; Lynden-Bell, R. M. A Molecular Dynamics Study of Carbon Dioxide in Water: Diffusion, Structure and Thermodynamics. *Mol. Phys.* **1998**, *94*, 963–972.
- (9) Ahadi, E.; Konermann, L. Ejection of Solvated Ions from Electrosprayed Methanol/Water Nanodroplets Studied by Molecular Dynamics Simulations. *J. Am. Chem. Soc.* **2011**, *133*, 9354–9363.
- (10) Liger-Belair, G.; Prost, E.; Parmentier, M.; Jeandet, P.; Nuzillard, J.-M. Diffusion Coefficient of CO₂ Molecules as Determined by ¹³C NMR in Various Carbonated Beverages. *J. Agric. Food Chem.* **2003**, *51*, 7560–7563.
- (11) Hess, B.; Kutzner, C.; van der Spoel, D.; Lindahl, E. GROMACS 4: Algorithms for Highly Efficient, Load-Balanced, and Scalable Molecular Simulation. *J. Chem. Theory Comput.* **2008**, *4*, 435–447.
- (12) Brooks, B. R.; Brooks, C. L.; MacKerell, A. D.; Nilsson, L.; Petrella, R. J.; Roux, B.; Won, Y.; Archontis, G.; Bartels, C.; Boresch, S.; et al. CHARMM: The Biomolecular Simulation Program. *J. Comput. Chem.* **2009**, *30*, 1545–1614.
- (13) Carroll, J. J.; Slupsky, J. D.; Mather, A. E. The Solubility of Carbon Dioxide in Water at Low Pressure. *J. Phys. Chem. Ref. Data* **1991**, *20*, 1201–1209.
- (14) Autret, G.; Liger-Belair, G.; Nuzillard, J.-M.; Parmentier, M.; Dubois de Montreynaud, A.; Jeandet, P.; Doan, B.-T.; Beloeil, J.-C. Use of Magnetic Resonance Spectroscopy for the Investigation of the CO₂ Dissolved in Champagne and Sparkling Wines: A Nondestructive and Unintrusive Method. *Anal. Chim. Acta* **2005**, *535*, 73–78.
- (15) Liger-Belair, G. How Many Bubbles in Your Glass of Bubbly? *J. Phys. Chem. B* **2014**, *118*, 3156–3163.
- (16) Berendsen, H. J. C.; Grigera, J. R.; Straatsma, T. P. The Missing Term in Effective Pair Potentials. *J. Phys. Chem.* **1987**, *91*, 6269–6271.
- (17) Mahoney, M. W.; Jorgensen, W. L. A Five-Site Model for Liquid Water and the Reproduction of the Density Anomaly by Rigid, Nonpolarizable Potential Functions. *J. Chem. Phys.* **2000**, *112*, 8910.
- (18) Mahoney, M. W.; Jorgensen, W. L. Diffusion Constant of the TIP5P Model of Liquid Water. *J. Chem. Phys.* **2001**, *114*, 363.
- (19) Liger-Belair, G. The Physics Behind the Fizz in Champagne and Sparkling Wines. *Eur. Phys. J.: Spec. Top.* **2012**, *201*, 1–88.
- (20) Siddiqi, M. A.; Lucas, K. Correlations for Prediction of Diffusion in Liquids. *Can. J. Chem. Eng.* **1986**, *64*, 839–843.
- (21) Taylor, R. *Multicomponent Mass Transfer*; Wiley Series in Chemical Engineering; Wiley: New York, 1993.
- (22) Chandler, D. Interfaces and the Driving Force of Hydrophobic Assembly. *Nature* **2005**, *437*, 640–647.
- (23) Liger-Belair, G.; Parmentier, M.; Jeandet, P. Modeling the Kinetics of Bubble Nucleation in Champagne and Carbonated Beverages. *J. Phys. Chem. B* **2006**, *110*, 21145–21151.